

**Key Points:**

- We developed a model parameterization approach to integrate functional gene data with CH_4 models
- Genome-enabled model parameterization enhanced model performance in simulating CH_4 cycling at a seasonal scale
- Genome-enabled model parameterization establishes more robust associations between CH_4 production and environmental conditions

Supporting Information:

Supporting Information may be found in the online version of this article.

Correspondence to:

X. Xu and L. Sun,
 xxu@sdsu.edu;
 sunli@iga.ac.cn

Citation:

Zuo, Y., He, L., Wang, Y., Liu, J., Wang, N., Li, K., et al. (2024). Genome-enabled parameterization enhances model simulation of CH_4 cycling in four natural wetlands. *Journal of Advances in Modeling Earth Systems*, 16, e2023MS004139. <https://doi.org/10.1029/2023MS004139>

Received 20 NOV 2023

Accepted 5 SEP 2024

Genome-Enabled Parameterization Enhances Model Simulation of CH_4 Cycling in Four Natural Wetlands

Yunjiang Zuo¹ , Liyuan He² , Yihui Wang², Jianzhao Liu¹, Nannan Wang¹, Kexin Li^{1,3}, Ziyu Guo¹, Lihua Zhang⁴, Ning Chen¹, Changchun Song¹, Fenghui Yuan¹, Li Sun¹, and Xiaofeng Xu² 

¹State Key Laboratory of Black Soils Conservation and Utilization, Northeast Institute of Geography and Agroecology, Chinese Academy of Sciences, Changchun, China, ²Biology Department, San Diego State University, San Diego, CA, USA,

³University of the Chinese Academy of Sciences, Beijing, China, ⁴College of Life and Environmental Sciences, Minzu University of China, Beijing, China

Abstract Microbial processes are crucial in producing and oxidizing biological methane (CH_4) in natural wetlands. Therefore, modeling methanogenesis and methanotrophy is advantageous for accurately projecting CH_4 cycling. Utilizing the CLM-Microbe model, which explicitly represents the growth and death of methanogens and methanotrophs, we demonstrate that genome-enabled model parameterization improves model performance in four natural wetlands. Compared to the default model parameterization against CH_4 flux, genomic-enabled model parameterization added another constraint on microbial biomass, notably enhancing the precision of simulated CH_4 flux. Specifically, the coefficient of determination (R^2) increased from 0.45 to 0.74 for Sanjiang Plain, from 0.78 to 0.89 for Changbai Mountain, and from 0.35 to 0.54 for Sallie's Fen, respectively. A drop in R^2 was observed for the Dajiuju nature wetland, primarily caused by scatter data points. Theil's coefficient (U) and model efficiency (ME) confirmed the model performance from default parameterization to genome-enabled model parameterization. Compared with the model solely calibrated to surface CH_4 flux, additional constraints of functional gene data led to better CH_4 seasonality; meanwhile, genome-enabled model parameterization established more robust associations between simulated CH_4 production rates and environmental factors. Sensitivity analysis underscored the pivotal role of microbial physiology in governing CH_4 flux. This genome-enabled model parameterization offers a valuable promise to integrate fast-cumulating genomic data with CH_4 models to better understand microbial roles in CH_4 in the era of climate change.

Plain Language Summary Soil microbes are the real engines for producing and oxidizing biological CH_4 in natural wetlands. However, most existing models do not explicitly simulate the dynamics of methanogens and methanotrophs, the microbial functional groups responsible for CH_4 production and oxidation. This study illustrates that genome-enabled model parameterization notably enhances model performance by comparing model versions with and without parameter optimization against functional gene data for methanogenesis and methanotrophy in four natural wetlands. In contrast to models solely calibrated to surface CH_4 flux, the additional constraint of the functional gene data improved the model performance in CH_4 at a seasonal level. This study proved that fast-cumulating gene data functional gene data could add value to microbial models.

1. Introduction

Methane (CH_4) is the second most potent greenhouse gas (Forster, 2007), contributing to approximately 25% of the human-induced radiative warming over the past century (IPCC, 2021). A minor increase in CH_4 emissions from terrestrial ecosystems might cause disproportionately profound impacts on climate warming (Kirschke et al., 2013). Natural wetlands are a significant source of CH_4 emissions (Melton et al., 2013; Tootchi et al., 2019), accounting for 62% of total biological CH_4 emissions in terrestrial ecosystems (Nazaries et al., 2013). Therefore, understanding CH_4 cycling in natural wetlands has profound implications for improving the predictions of terrestrial CH_4 emissions to the atmosphere.

The CH_4 fluxes in wetlands depend on the balance between microbial methanogenesis and methanotrophy (Fazli et al., 2013). In particular, changes in the composition of methanogens and their spatial dynamics play crucial roles but are often overlooked in estimating CH_4 production in natural wetlands (Kharitonov et al., 2021). Functional gene data provide insights to distinguish CH_4 -producing bacteria from CH_4 -oxidizing bacteria and

enable the identification of different functional types of CH_4 -producing bacteria and CH_4 -oxidizing bacteria, thereby providing a better understanding of their contributions within ecosystems (Bajic & Sanchez, 2020). As emphasized in previous research, microbial functional gene data hold significant potential for improving CH_4 microbial models (Nazaries et al., 2013; Xu, Riley, et al., 2016). Such data facilitate the differentiation of the abundance of various methanogens, thereby providing insights into CH_4 processes in diverse wetland environments (Bajic & Sanchez, 2020). Moreover, functional gene data can effectively distinguish CH_4 production pathways, thus revealing the specific functions of microbial communities in the CH_4 processes (Wang, Zhu, et al., 2022). In summary, as microorganisms play a central role in CH_4 cycling, identifying how microbial processes might underpin variability in CH_4 production may further improve our ability to understand, represent, and predict wetland CH_4 cycling globally (Chen et al., 2020). Nevertheless, the diversity of microbial communities and the varying dominance of species in different ecosystems engaged in CH_4 cycling adds to the complexity of genome-enabled parameterization (Kharitonov et al., 2021).

Although the archeal and bacterial taxa responsible for methanogenesis and methanotrophy are increasingly well-defined, these microbial communities are often underrepresented in CH_4 models (Arnold et al., 2023; Xu, Yuan, et al., 2016). Recently, growing focus has been placed on integrating microbial processes into terrestrial ecosystem models (Sulman et al., 2014; Walker et al., 2018; Xu et al., 2014). Several CH_4 models have indeed integrated microbial processes, such as JULES-Microbe (Chadburn et al., 2020), XPTEM-XHAM (Oh et al., 2020), ELM-SPRUCE (Ricciuto et al., 2021; Yuan, Wang, Ricciuto, Shi, Yuan, et al., 2021; Yuan, Wang, Ricciuto, Shi, Hanson, et al., 2021), and CLM-Microbe (Wang et al., 2019, 2022b; Xu et al., 2015). These models merely incorporate microbial processes into the model to distinguish CH_4 production and CH_4 oxidation pathways, using empirically derived parameters, without validating the individual CH_4 process. Model-data fusion methods have recently been employed to assess wetland CH_4 emissions (Sharp et al., 2024). This approach uses observational data to constrain process models that are difficult to calibrate and can be used to evaluate CH_4 cycling processes (Ueyama et al., 2023).

To explore the impact of genome-driven parameterization in the CH_4 model and deepen our understanding of microbial mechanisms involved in CH_4 cycling, we aimed to integrate functional gene data with the CLM-Microbe model, specifically focusing on different methanogenic processes. Simulations were run for four sites (the Sanjiang Plain, Changbai Mountain, Dajiuju Peatland, and Sallie's Fen) with meteorology, gross primary productivity (GPP), CH_4 flux, and gene data. Our primary objectives encompass three key aspects: (a) to develop a model parameterization approach to integrate genomic data with a CH_4 model, (b) to compare the simulated CH_4 between simulations conducted with and without gene data, and (c) to gain a better understanding of the microbial mechanisms of various methanogenesis pathways.

2. Methodology

2.1. Site Description

This study selected four wetland ecosystems: the Sanjiang Plain, Changbai Mountain, Dajiuju Peatland, and Sallie's Fen. The sites were chosen based on data availability for practical analysis and comparison, as well as previous studies, connecting the research to existing literature and providing additional comparative standards for results (Zuo et al., 2022). The Sanjiang Plain is located in northeast China (47.58°N , 133.52°E). The climate is characterized by a continental monsoon regime. It has a mean annual temperature (MAT) of 2.52°C and a mean annual precipitation (MAP) of 558 mm. This wetland represents a freshwater marshland wetland type. The wetland in Changbai Mountain (42.35°N , 126.38°E) is characterized by a continental monsoon climate, with a MAT of 3.3°C and a MAP of 1,054 mm. It falls into the category of cold temperate mountain peatland wetland type. The dominant plant community consists of moss species. This wetland is characterized by a Holocene peat layer measuring 4–5 m deep, primarily moss peat. The Dajiuju peatland is situated in southern China (31.47°N , 110.00°E). It has a temperate monsoon climate with a MAT of 10°C and a MAP ranging from 1,200 to 1,500 mm. This peatland falls into temperate peatland wetland type category. Sallie's Fen site (43.21°N , 71.06°W), which is a poor fen located in Barrington, New Hampshire, USA, has a continental climate with cold winters and warm summers, with MAT ranging from 5°C to 10°C . Its MAP is approximately 1,000–1,400 mm, and its dominant vegetation is sedge.

Table 1Site Information and Data Sources of Atmospheric Forcing Data and Observations (GPP, CH_4 Flux, Methanogens Biomass)

Site	Location	Data	Resolution	Year	Source
Sanjiang Plain	47.58°N, 133.52°E	Atmospheric forcing	1 km × 1 km	2005–2018	Sanjiang Plain Marsh Wetland Ecological Experimental Station (http://sjm.cern.ac.cn/meta/metaData)
		GPP	Daily	2012–2020	
		CH_4	Daily	2012–2020	
		Gene data	Depth of 10 cm	2019–2020	
Changbai Mountain	42.35°N, 126.38°E	Atmospheric forcing	0.1 × 0.1°	2003–2018	China Meteorological Forcing Dataset (https://data.tpdc.ac.cn/)
		GPP	Daily	2011	(Cao, 2015)
		CH_4	Daily	2011	(Shi, 2019)
		Gene data	Depth of 10 cm	2011	(Shi, 2019)
Daijihu Peatland	31.50°N, 110.00°E	Atmospheric forcing	0.1 × 0.1°	2010–2018	China Meteorological Forcing Dataset
		GPP	Daily	2019–2021	MODIS (https://lpdaac.usgs.gov/products/mod17a2hv006/)
		CH_4	Monthly	2016, 2019	(Liu et al., 2021)
		Gene data	Depth of 20 cm	2019	(Liu et al., 2021)
Sallie	43.51°N, 71.05°W	Atmospheric forcing	0.5 × 0.5°	2000–2016	CRUNCEP Version 7 dataset
		GPP	Daily	2010	MODIS
		CH_4	Daily	2008–2011	(Noyce et al., 2014)
		Gene data	Depth of 20 cm	2014	(Perryman et al., 2022)

2.2. Model Description

The CLM-Microbe model branches from the framework of default CLM4.5 by developing a microbial functional group-based module for CH_4 production and consumption (Xu et al., 2015) and a framework of microbial C assimilation (Xu et al., 2014). It incorporates mechanisms of dissolved organic carbon (DOC) fermentation, hydrogenotrophic methanogenesis, acetoclastic methanogenesis, aerobic methanotrophy, anaerobic methanotrophs, and H_2 production (He et al., 2021a, 2021b; Wang et al., 2019; Xu et al., 2015; Zuo et al., 2022). Detailed mathematical expressions for CH_4 production and consumption processes were described by Xu et al. (2015). We introduce the major governing equation of CH_4 processes in CLM-Microbe in Supporting Information. The codes of the CLM-Microbe model have been archived on GitHub (<https://github.com/email-clm/CLM-Microbe>). The model version used in this study was checked out from GitHub on 27 May 2020.

2.3. Model Forcing Data

Model forcing data include air temperature, relative humidity, wind speed, atmospheric pressure, precipitation, incoming longwave radiation, and shortwave radiation. The Sanjiang Plain simulation was driven by the climate data from the Sanjiang field observation station with a resolution of 1 km × 1 km, and organized into hourly datasets. For the Changbai Mountain and Daijihu Peatland simulations, we used the Chinese atmospheric forcing dataset (CMFD) with a resolution of 0.1 × 0.1° and divided into hourly time steps. For Sallie's Fen simulation, we used the CRUNCEP Version 7 dataset for the Community Land Model that is set on a 0.5 × 0.5° global grid and is divided into hourly time steps (Table 1).

2.4. Functional Gene Data for Methanogenesis

We collected microbial functional gene data for four seasons at four sites. The microbial functional gene data collected in the Sanjiang Plain were from a soil profile of 100 cm and a resolution of 10 cm. The data were collected during October 10–12, 2019, December 27–29, 2019, May 13–15, 2020, and July 19–21, 2020, representing autumn, winter, spring, and summer, respectively (Wang, Zhu, et al., 2022). The functional gene data from the other three sites across four seasons were compiled from published literature; they represented a depth of 60 cm and a resolution of 10 cm, 20 cm, and 20 cm, respectively (Liu et al., 2021; Perryman et al., 2022; Shi, 2019). Microbial functional gene data were obtained through two distinct sequencing methods: metagenomic sequencing for the Sanjiang Plain and 16S rRNA sequencing for the other three sites. Both techniques provide valid information for distinguishing the relative abundance of different methanogens within the wetland

ecosystems. In the metagenomic sequencing of the Sanjiang Plain, we utilized modules M00357 and M00567 to represent the acetate and hydrogenotrophic CH_4 metabolic pathways, respectively. The vertical relative trends of these metabolic pathways are employed to characterize the vertical relative trends of acetate and hydrogenotrophic methanogenesis abundance. This study utilized the gene data collected from Changbai Mountain, Dajiuju Peatland, and Sallie's Fen, which were analyzed using 16S rRNA sequencing in combination with *mcrA* gene primers (e.g., 338F and 806R) to characterize CH_4 -producing microbial communities (Liu et al., 2021; Perryman et al., 2022; Shi, 2019). We differentiated acetoclastic and hydrogenotrophic methanogens based on microbial metabolic characteristics (utilization of acetate or H_2/CO_2), aiming to infer the relative abundance variations of acetoclastic and hydrogenotrophic methanogens along the vertical spatial gradient (Kalyuzhnaya et al., 2019).

In this study, we employed the functional gene data to validate the model using relative trends rather than absolute values, as relative trends better reflect variations under different conditions, thus minimizing errors while processing genetic abundance data. To achieve this, we computed the averages of the relative abundance of acetoclastic and hydrogenotrophic methanogens across four seasons at each site. Subsequently, we standardized these averages to calculate the annual trends in methanogen variation with depth. To validate model accuracy, we calibrated parameters related to methanogen growth and mortality (*GrowRH2Methanogens*, *DeadRH2Methanogens*, *YH2Methanogens*, *GrowRAceMethanogens*, *DeadRAceMethanogens*, *YAceMethanogens*, see Supporting Information equations (7)–(11)). Finally, we standardized the model-simulated results for both methanogen types to facilitate comparison with observed values.

2.5. Model Implementation

In our previous research, we validated the CLM-Microbe model in simulating CH_4 flux and further examined the model performance in three typical wetlands in Northeast China (Zuo et al., 2022). In this study, we further expanded our previous study by including more sites and optimizing the parameters for parameterizing the model in simulating methanogens and methanotrophs. We selected 15 critical parameters for model parameterization as those parameters primarily control the decomposition of soil organic C, CH_4 production and oxidation, and microbial physiology (Table S1 in Supporting Information S1).

To identify the role of gene data in CH_4 dynamics, we conducted model simulations for each site using two different configurations: default CLM-Microbe (without gene data) and parameterized CLM-Microbe (with gene data) models. We set up model simulations for each site using the CLM-Microbe model. The model implementation was carried out in three stages for all sites. First, the accelerated model spin-up was set up for 2,000 years to allow the system to accumulate C. Then a final spin-up was set up for 50 years to enable the ecosystem to reach a state with the realistic decomposition rates before the transient simulations that cover the period of 1850–2019 (Koven et al., 2013; Thornton & Rosenbloom, 2005). Since observational CH_4 fluxes are reported daily, we maintained a consistent daily time step for the output resolution of transient simulations.

For the default CLM-Microbe model simulations, the parameters were set to be the default parameter in Xu et al. (2015) and Zuo et al. (2022); it was performed within their ranges to determine the optimal values of parameters in the CH_4 module for simulating the observational gross primary productivity (GPP) and CH_4 flux for each site. For the parameterization of the CLM-Microbe model, the model parameterization was initialized with the values of the default CLM-Microbe model for each site; subsequently, gene data were utilized to parameterize the CH_4 microbial module. We primarily focused on the parameters related to decomposition of soil organic C (*KAce*, *AceProdACmax*), CH_4 production and oxidation, and microbial physiology (e.g., *GrowRH2Methanogens*, *DeadRH2Methanogens*, *YH2Methanogens*, *GrowRAceMethanogens*, *DeadRAceMethanogens*, *YAceMethanogens*). These parameters were set as the default values according to Xu et al. (2015). The experiment was performed within their specified ranges to determine the optimal parameter values in the microbial module for simulating the observed CH_4 flux and microbial biomass at each site.

We validated the model for the Sanjiang Plain wetland using GPP and CH_4 flux observation data spanning from 2012 to 2020, along with gene data collected from 2019 to 2020. For the Changbai Mountain site, we extracted GPP and CH_4 flux data from Cao (2015) for the year 2011 and validated the biomass of methanogens in the model using gene data from the same year (Shi, 2019). For the Dajiuju peatland, we obtained GPP data from the MODIS dataset from 2019 to 2021 and extracted CH_4 flux and gene data from Liu et al. (2021). Similarly, we used MODIS data in the year 2010 to validate GPP for Sallie's Fen, whereas validated CH_4 flux data from 2008 to 2011

and microbial biomass with microbial data from 2014 were obtained from the literature for model validation (Noyce et al., 2014; Perryman et al., 2022). We calculated the correlation between CH_4 production rate and environmental factors with different parameterization methods to quantify these relationships.

2.6. Model Evaluation and Sensitivity Analysis

To evaluate the model performance regarding GPP and CH_4 flux, we used error statistics to quantify the difference between the modeled results and observational data. Simple linear regression was used to analyze the relationship between observed and simulated values. To estimate the accuracy of the model, we used three accuracy evaluation indicators: coefficient of determination (R^2), root mean square error (RMSE), mean absolute error (MAE), modeling efficiency (ME), and Theil's inequality coefficient (U). To investigate the impact of genome-enabled parameterization on the methanogenesis process in microorganisms, we performed simple linear regression analyses to examine the relationship between the rates of acetoclastic methanogenesis and hydrogentrophic methanogenesis with soil temperature, moisture, atmospheric temperature, and precipitation. The R^2 was used to evaluate the overall performance of the model before and after genomic-enabled parameterization optimization.

$$R^2 = \frac{\sum_{i=1}^n (y_i - \hat{y}_i)^2}{\sum_{i=1}^n (y_i - \bar{y})^2}$$

$$RMSE = \sqrt{\frac{\sum_{i=1}^n (y_i - \hat{y}_i)^2}{n}}$$

$$MAE = \frac{\sum_{i=1}^n |y_i - \hat{y}_i|}{n}$$

$$ME = 1 - \frac{\sum (y_i - \hat{y}_i)^2}{\sum (y_i - \text{mean}(\hat{y}_i))^2}$$

$$U = \sqrt{\frac{\sum_{i=1}^n (y_i - \hat{y}_i)^2}{\sum_{i=1}^n y_i^2}}$$

Where y_i is the observed value; \hat{y}_i means the simulated value; $\text{mean}(\hat{y}_i)$ indicates the mean of the simulated value; n is the number of data points. The MAE indicates the mean error of the model simulation, and thus smaller MAE values suggest better model performance. The $RMSE$ quantifies the mean error of model simulation with low values indicating high model accuracy. R^2 indicates the general performance of the model. Parameter U is *Theil's* inequality coefficient (Blanco et al., 2007; Theil, 1966), and it could be 0 or greater. $U = 0$ means he perfect fit between the model results and observations; larger U value means poorer model performance. $ME = 1$ indicates a perfect fit. $ME = 0$ reveals that the model is no better than a simple average, and negative values indicate poor performance.

A global sensitivity analysis was conducted for each wetland type to identify the most critical process and parameters for CH_4 and microbial dynamics. We focused on the 15 parameters related to plant and microbial processes critical for microbial biogeochemistry (Table S2 in Supporting Information S1). We set up model simulations for each parameter with $+20\%$ and -20% changes and investigated the responses of the modeled CH_4 microbial biomass and CH_4 flux. The index S , comparing the change in the model output relative to the model response for a nominal set of parameters, was calculated based on the following equation (Xu et al., 2015):

$$S = \frac{(Ra - Rn)/Rn}{(Pa - Pn)/Pn}$$

where S is the ratio of the standardized change in model response to the standardized change in parameter values. Ra and Rn are model responses for altered and nominal parameters, respectively, and Pa and Pn are the altered

Table 2

Default Values and Final Optimization Values of Eight Key Parameters Related to the Methanogenesis Process for Four Sites

Parameter	Sanjiang plain		Changbai mountain		Daijihu peatland		Sallie's fen	
	Default value	Optimized value	Default value	Optimized value	Default value	Optimized value	Default value	Optimized value
<i>KAce</i>	64	64	32	32	32	16	45	64
<i>AceProdACmax</i>	6e-6	6e-6	2e-6	5e-6	3e-6	6e-7	0.00005	1e-5
<i>GrowRH2Methanogens</i>	0.01	0.2	0.03	0.1	0.1	0.2	1e-6	1e-6
<i>DeadRH2Methanogens</i>	0.001	1e-6	0.0001	0.0001	0.00001	0.00001	1e-7	1e-8
<i>YH2Methanogens</i>	0.015	0.1	0.01	0.01	0.01	0.01	1e-4	1e-4
<i>GrowRAceMethanogens</i>	0.008	0.05	0.1	0.1	0.1	0.15	1e-6	1e-5
<i>DeadRAceMethanogens</i>	0.002	2e-6	0.0002	0.0001	0.00001	1e-6	9e-6	9e-5
<i>YAceMethanogens</i>	0.2	0.1	0.2	0.00001	0.1	0.01	1e-7	1e-6

Note. Light red indicates parameter values increasing, light blue indicates parameter values decreasing, and blank represents no change.

and nominal parameters, respectively. S is negative if the direction of the model response opposes the direction of parameter change (Wang et al., 2019; Xu et al., 2015; Yuan et al., 2021a, 2021b).

3. Results

3.1. Parameter Optimization With Functional Gene Data

We conducted the parameterization of the CH_4 module using gene data and optimized the parameters for CH_4 -related microbial processes (Table 2). These parameters primarily govern substrate decomposition and the growth and death rates of CH_4 -related microbes. Compared with default parameter values, changes in major parameters were observed in the Sanjiang Plain. Specifically, the growth rate and efficiency parameters (*GrowRH2Methanogens* and *YH2Methanogens*, respectively) for hydrogenotrophic methanogens increased by 0.19 and 0.085, respectively, while the death rate (*DeadRH2Methanogens*) decreased. These changes resulted in a 52% increase in the CH_4 production rate of hydrogenotrophic methanogens (Figure 1a). In the case of the Changbai Mountain, the optimization process led to an increase in the growth rate for hydrogenotrophic methanogens (*GrowRH2Methanogens*) and a 50% reduction in the death rate for acetoclastic methanogens (*DeadRAceMethanogens*). Furthermore, the maximum rate of acetoclastic CH_4 production (*AceProdACmax*) increased, leading to a higher CH_4 production rate for both methanogens than the default values (Figure 1b). In the Daijihu peatland, we observed a 50% reduction in the half-saturation coefficient (*KAce*) of available carbon and a 80% reduction in the maximum acetate production rate (*AceProdACmax*). Simultaneously, the growth rates for both methanogens

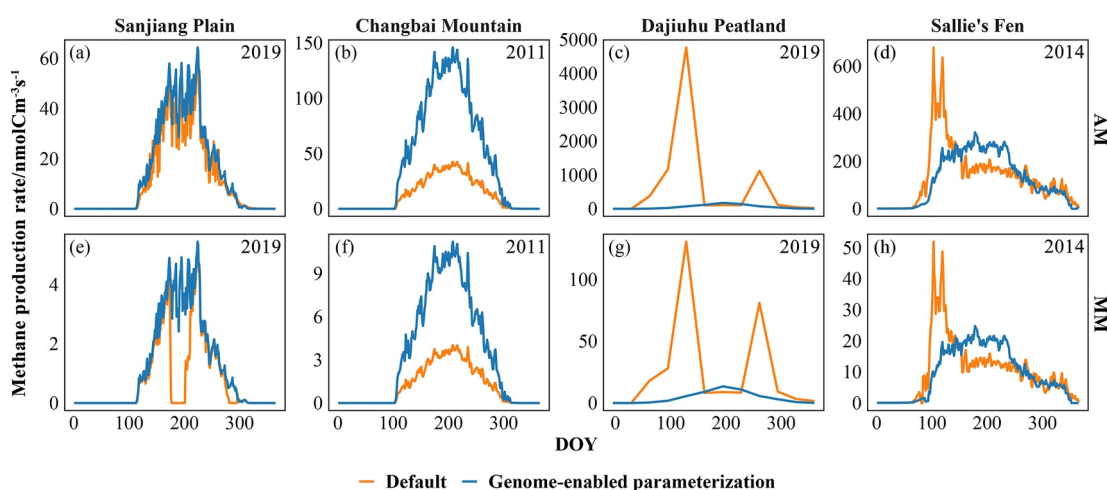


Figure 1. Simulation of CH_4 production rate in different methanogenesis pathways (AM: Acetoclastic methanogenesis, MM: Hydrogenotrophic methanogenesis). (a), (e) Sanjiang Plain, (b), (f) Changbai Mountain, (c), (g) Daijihu Peatland, (d), (h) Sallie's Fen. DOY: day of year.

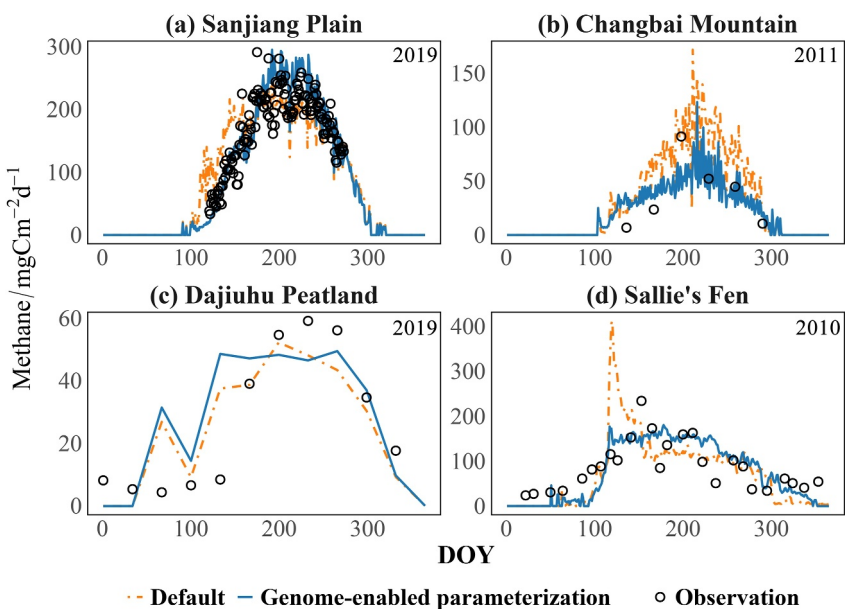


Figure 2. Observed and modeled CH_4 . (a), Sanjiang Plain (b), Changbai Mountain (c), Dajiuju Peatland (d), Sallie's Fen. DOY: day of year.

(*GrowRH2Methanogens* and *GrowRAceMethanogens*, respectively) increased. These adjustments resulted in a smoother seasonal variation trend for the CH_4 production rate of the two methanogenesis (Figure 1c). For Sallie's Fen, the microbial growth and death rates were calibrated to lower values than the other three sites. A comparison revealed that *AceProdACmax* and *DeadRH2Methanogens* parameters decreased, while the values of *KAce*, *GrowRAceMethanogens*, *DeadRAceMethanogens*, and *YAceMethanogens* increased. These changes reduced the seasonal fluctuations of CH_4 production rates for both methanogenic pathways (Figure 1d).

3.2. Comparison of Simulated CH_4 Flux With and Without Genomic-Enabled Parameterization

The CLM-Microbe model effectively captures the dynamic of CH_4 fluxes (Figure 2) and the observed GPP (Figure S1 in Supporting Information S1). Compared with simulation results with the default parameters, the accuracy of CH_4 flux simulated with the optimized parameters at all sites was enhanced, but genome-driven parameterization minimally influenced GPP. The R^2 values of CH_4 flux at all sites exceeded 0.5, among which the R^2 values for Sanjiang Plain, Changbai Mountain, Dajiuju Peatland, and Sallie's Fen were 0.74, 0.89, 0.78, and 0.54, respectively (Table 3). Furthermore, the R^2 values increased for most sites after parameterization, except for Dajiuju peatland. Specifically, the R^2 values increased by 0.29, 0.11, and 0.19 for Sanjiang Plain, Changbai Mountain, and Sallie's Fen, respectively, while the R^2 value decreased by 0.13 for Dajiuju Peatland.

The optimized parameterization improved simulation accuracy, with substantial reductions in RMSE and MAE values observed, especially in the Sanjiang Plain, Changbai Mountain, and Sallie's Fen. Specifically, the RMSE values decreased from 0.18, 0.25, and 0.33 to 0.14, 0.18, and 0.23, for Sanjiang Plain, Changbai Mountain, and Sallie's Fen, respectively. Correspondingly, the MAE values decreased from 0.15, 0.14, and 0.26 to 0.11, 0.11, and 0.17 (Table 3). The ME values for the genome-enabled parameterization across sites like Sanjiang Plain (0.61) and Sallie's Fen (0.72) demonstrate the robustness of model, indicating a considerable improvement over default modeling. A resulting $U = 0$ meant a perfect fit between the model results and observations; a larger U value meant poorer model performance (Blanco et al., 2007). The genome-enabled parameterization results in relatively low U values (Sanjiang Plain: 0.11, Changbai Mountain: 0.27, and Sallie's Fen: 0.31), reflecting good alignment between modeled and observed CH_4 flux. Theil's U values for both parameterizations are relatively low (0.28 for genome-driven and 0.21 for default).

The genome-enabled parameterization method estimated annual CH_4 emissions ranging from 7.62 to 30.52 $\text{g} \cdot \text{m}^{-2} \cdot \text{a}^{-1}$ among sites, whereas the default parameterization yields estimated ranging from 9.06 to 30.79 $\text{g} \cdot \text{m}^{-2} \cdot \text{a}^{-1}$ among sites. Interestingly, genome-driven parameterization showed that the highest annual CH_4

Table 3*Site Level Evaluation of the Goodness-Of-Fit Criteria Computed for the Simulated CH_4 Flux ($gC/m^2/d$)*

Sites	Genome-driven parameterization					Default parameterization				
	R^2	RMSE	MAE	U	ME	R^2	RMSE	MAE	U	ME
Sanjiang Plain	0.74	0.14	0.11	0.11	0.61	0.45	0.18	0.15	0.15	0.32
Changbai Mountains	0.89	0.18	0.11	0.27	0.25	0.78	0.25	0.14	0.28	-0.12
Dajiuju	0.78	0.21	0.15	0.28	0.43	0.91	0.11	0.09	0.21	0.55
Sallie	0.54	0.23	0.17	0.31	0.72	0.35	0.33	0.26	0.32	0.15

Note. MAE, mean absolute error; RMSE, root mean square error; R^2 , R square. MAE and RMSE values indicate the mean error of the model; smaller values represent higher model performance. R^2 values mean the proportion of variation explained by the model; higher R^2 values indicate better model performance; Theil's inequality coefficient (U): Parameter U could be 0 or greater than 1. A resulting $U = 0$ meant a perfect fit between the model results and observations; a larger U value meant poorer model performance; Modeling efficiency (ME): A resulting ME = 1 indicated a perfect fit, ME = 0 reveals that the model was no better than a simple average, and negative values indicated poor performance.

emissions were observed in the Sanjiang Plain, while the lowest was in the Changbai Mountain site. Conversely, the default simulation indicated that the Dajiuju peatlands exhibit the lowest annual CH_4 emissions. Compared to the default parameterization results, the genome-driven parameterization showed that CH_4 emissions for the Sanjiang Plain and Changbai Mountain decreased by 0.27 and 4.47 $g \cdot m^{-2} \cdot a^{-1}$, respectively, while the CH_4 emissions for the Dajiuju Peatland and Sallie's Fen increased by 1.12 and 1.33 $g \cdot m^{-2} \cdot a^{-1}$, respectively.

3.3. Vertical Distribution of Methanogens and Methanotrophs

Compared to the default simulation, the gene data-parameterized CLM-Microbe model captured vertical variations in the biomass of methanogens that were consistent with the overall trend of the observed values (Figure 3, Figure S3 in Supporting Information S1). In the Sanjiang Plain, we observed a decreasing trend in the biomass of both methanogens along the soil profile, with a notably higher biomass of acetoclastic methanogens (AM) compared to hydrogenotrophic methanogens (MM). At the Changbai Mountain site, the biomass of AM increased with depth, reaching a stable level below 30 cm, while the biomass of MM exhibited a declining trend with depth and stabilized below 30 cm. In contrast, in the Dajiuju peatland and Sallie's Fen, AM biomass exhibited an overall decreasing trend with depth, while MM biomass showed an increasing trend. Overall, the model predictions of methanogen biomass variations with depth align with the observed patterns.

In the surface layer of the Sanjiang Plain wetland, the biomass of methanotrophs was relatively lower than in the deeper layers (Figure S2). As the depth increased, the biomass of anaerobic methanotrophs (AOM) exhibited an initial increase followed by a decrease. In contrast, the biomass of aerobic methanotrophs (OM) showed an increasing trend with depth. In the Changbai Mountain peatland, there was an overall decrease in AOM biomass with depth, while the biomass of OM increased with depth. The Dajiuju peatland and Sallie's Fen exhibited a

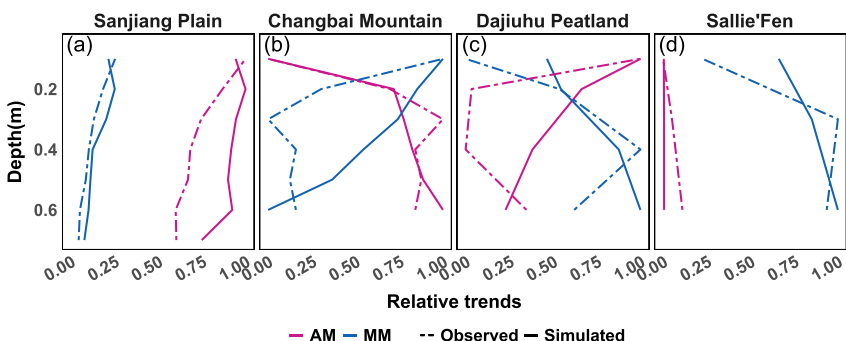


Figure 3. Comparison between observed functional gene abundance and modeled methanogens microbial biomass along soil depth. (a) Sanjiang Plain, (b) Changbai Mountain, (c) Dajiuju Peatland, (d) Sallie's Fen. AM: Acetoclastic methanogenesis, MM: Hydrogenotrophic methanogenesis.

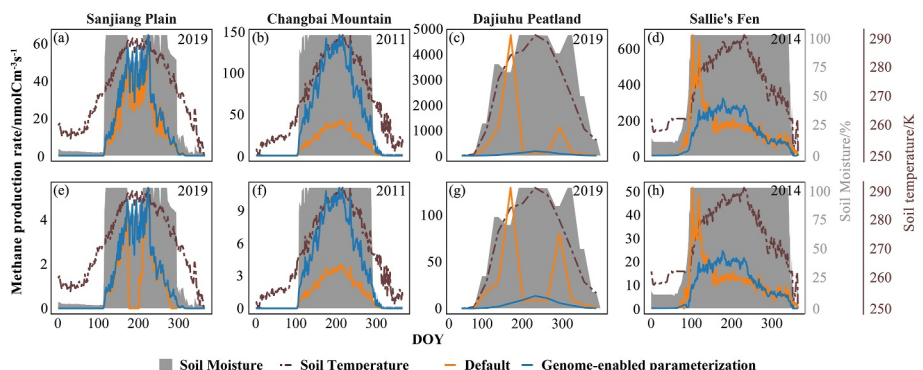


Figure 4. Soil temperature, soil water and simulation of CH_4 production rate in different methanogenesis pathways (AM: Acetoclastic methanogenesis, MM: Hydrogenotrophic methanogenesis). (a), (e), Sanjiang Plain (b), (f), Changbai Mountain (c), (g), Dajiuju Peatland (d), (h), Sallie's Fen. DOY: day of year. Orange represents the CH_4 production rate simulated by default parameters, blue represents the CH_4 production rate simulated by genomic-driven parameterization, brown line represents soil temperature, and dark gray represents soil moisture.

similar trend, where the biomass of both AOM and OM initially increased and then decreased with depth in the surface layer.

3.4. Environmental Factors and CH_4 Production Rates

The better model performance after genome-enabled parameterization is also advocated by the apparent seasonality in simulated CH_4 production rates and their association with environmental factors. Water content and temperature are essential factors affecting CH_4 emissions, and in this study, we selected air temperature, precipitation, soil temperature, and soil moisture as environmental factors. The seasonal patterns of CH_4 production rates, simulated with genome-driven parameterization, more closely align with the annual trends of environment factors than production rates from the default model (Figure 4, Figures S8 and S11 in Supporting Information S1). We calculated the correlation between CH_4 production rate and environmental factors with different parameterization methods to quantify these relationships. The outcomes of the acetoclastic CH_4 production rate and soil temperature correlation analysis revealed a slight increase in R^2 values for the Sanjiang Plain and Changbai Mountain compared with default parameterization. However, for the Dajiuju peatland and Sallie's fen, R^2 values increased by 0.60 and 0.66, respectively (Figure S4 in Supporting Information S1). Furthermore, compared with the default parameterization, the hydrogenotrophic CH_4 production rate and soil temperature correlation analysis indicate that R^2 values experienced noticeable increases with genome-driven parameterization for the Sanjiang Plain, Dajiuju peatland, and Sallie's Fen, with increments of 0.30, 0.55, and 0.65, respectively (Figure S5 in Supporting Information S1). The CH_4 production rate for Changbai Mountain displayed an approximately threefold increase compared to the default parameterization results (Figures 4b and 4f).

The correlation between the two CH_4 production rates and soil moisture content showed that in Dajiuju Peatland and Sallie's Fen, the R^2 values obviously increased (Figures S6 and S7 in Supporting Information S1). Specifically, for the acetoclastic CH_4 production rate, the R^2 values increased by 0.61 and 0.21, respectively, and for the hydrogenotrophic CH_4 production rate, the R^2 values increased by 0.57 and 0.21, respectively (Figures S6 & S7 in Supporting Information S1). The changes in the correlation between the CH_4 production rate and atmospheric temperature were similar to those with soil temperature (Figures S8, S9, & S10 in Supporting Information S1). Additionally, compared to the default parameterization results, only the R^2 value related to CH_4 production rate and precipitation increased in the Dajiuju peatland (Figures S11, S12, & S13 in Supporting Information S1). In contrast, the R^2 values for other sites remained relatively stable.

4. Discussion

4.1. Strengths of Using Gene Data to Parameterize the Model

This study used microbial functional gene data to parameterize a microbial explicit model—CLM-Microbe to simulate microbial mechanisms on CH_4 cycling in four natural wetlands. Compared to the default parameters of

the CLM-Microbe model, optimization through the integration of functional gene data with CH₄ models led to changes in parameters controlling the growth and mortality rates of CH₄-producing bacteria (Table 2). In the Sanjiang Plain, the growth rate (*GrowRH2Methanogens*) of hydrogenotrophic methanogens increased while the death rate (*DeadRH2Methanogens*) decreased, indicating an increase in the biomass of hydrogenotrophic methanogens, resulting in an increased CH₄ production rate via the hydrogenotrophic pathway (Figure 1e). The growth and death rate parameters of both CH₄-producing bacteria in Changbai Mountain, Dajiuju peatland, and Sallie's Fen were also verified through gene data (Figure 3), further optimizing the seasonal variation trends of CH₄ production rates and improving the accuracy of CH₄ flux simulations. Previous studies have shown that gene data can reveal the diversity of CH₄ microbial communities and elucidate different CH₄ production metabolic pathways (Wang, Yuan, et al., 2022). Model-data fusion methods have recently been used to assess wetland CH₄ emissions (Sharp et al., 2024; Ueyama et al., 2022). This approach utilizes observational data to constrain process models that are difficult to calibrate and can be used to evaluate CH₄ cycling processes (Ueyama et al., 2023). Microbial gene data holds immense potential in ecological modeling, as it can enhance model accuracy (Sulman et al., 2018).

We found that integrating gene data with models can improve the accuracy of CH₄ flux simulations, as evidenced by the increased R^2 values, decreased RMSE, and MAE values in between simulated and observed CH₄ flux in the Sanjiang Plain, Changbai Mountain, and Sallie's Fen (Table 3). The increase in R^2 values for the Sanjiang Plain, Changbai Mountain, and Sallie's Fen confirms the improved accuracy of the model simulations. The decrease in RMSE and MAE values indicates a reduction in model prediction errors, further corroborating the overall improvement in simulation accuracy. However, the increase in R^2 values for Changbai Mountain and Sallie's Fen was slightly lower compared to the Sanjiang Plain, and the R^2 value for Dajiuju peatland decreased. There may be several reasons for the relatively poor performance of the CLM-Microbe model at those sites. First, the available observational data were limited. Second, differences in measurement methods for the gene abundance of methanogens are also an important factor. The metagenomic sequencing method was used to measure gene abundance in Sanjiang Plain, while the 16S rRNA sequencing method was used in the other three sites. It is well-known that compared to metagenomic sequencing methods, 16S rRNA sequencing methods have limited resolution and can only provide limited taxonomic information, which may lead to errors in observational data and subsequently affect the verification results of CH₄-producing bacteria gene abundance (Church et al., 2020). Third, although microbial processes of CH₄ oxidation are included in our model, the lack of data on CH₄-oxidizing genes prevent the validation of methanotrophs biomass.

Previous research suggests that validated CH₄ models based on microbial functional groups can enhance our ability to estimate regional CH₄ budgets using the model and study the combined contributions of microbes and the environment to surface CH₄ flux (Kharitonov et al., 2021; Reid, 2011). This aligns with the findings of this study. The decrease in R^2 values for CH₄ flux in the Dajiuju Peatland may be due to the limited number of observed values (Table 3). This study accurately simulated the vertical trends in methanogen biomass (Figure 3), optimized the seasonal variations in different CH₄ production (Figure 1), and improved the accuracy of CH₄ flux simulations (Figure 2). Previous studies indicated that integrating gene data and models aids in a deeper understanding of the CH₄ cycling process. Methanogens in the soil significantly influence CH₄ emissions (Kroeger et al., 2021), and the CH₄ production process is a crucial factor in regulating CH₄ temporal patterns (Ricciuti et al., 2021). This aligns with the findings of this study. Environmental factors influence microbial CH₄ production processes, and this study reaffirms this by correlating simulated results from gene and model integration with environmental factors (Figure 4).

4.2. Key Parameters Controlling CH₄ Microbial Processes

In our analysis, the sensitivity results emphasize the critical role of parameters that govern substrate decomposition, microbial growth rates, and death rates in influencing CH₄ flux (Figure 5). Notably, acetate, a primary substrate in the CH₄ production process, significantly impacts CH₄ flux, a point well-established in previous studies (Dellagnezze et al., 2023; Hines et al., 2008). Our research echoes these findings by highlighting the importance of controlling acetate-related parameters (*KAce* and *AceProdACmax*) in governing CH₄ flux (Figure 5). For the simulations at the Changbai Mountain, Dajiuju peatland, and Sallie's Fen, we adjusted substrate-related parameters to optimize CH₄ production rates, which enhanced the accuracy of the simulated CH₄ flux (Table 2). Moreover, earlier models by researchers such as James (1993) and Segers (1998) have also

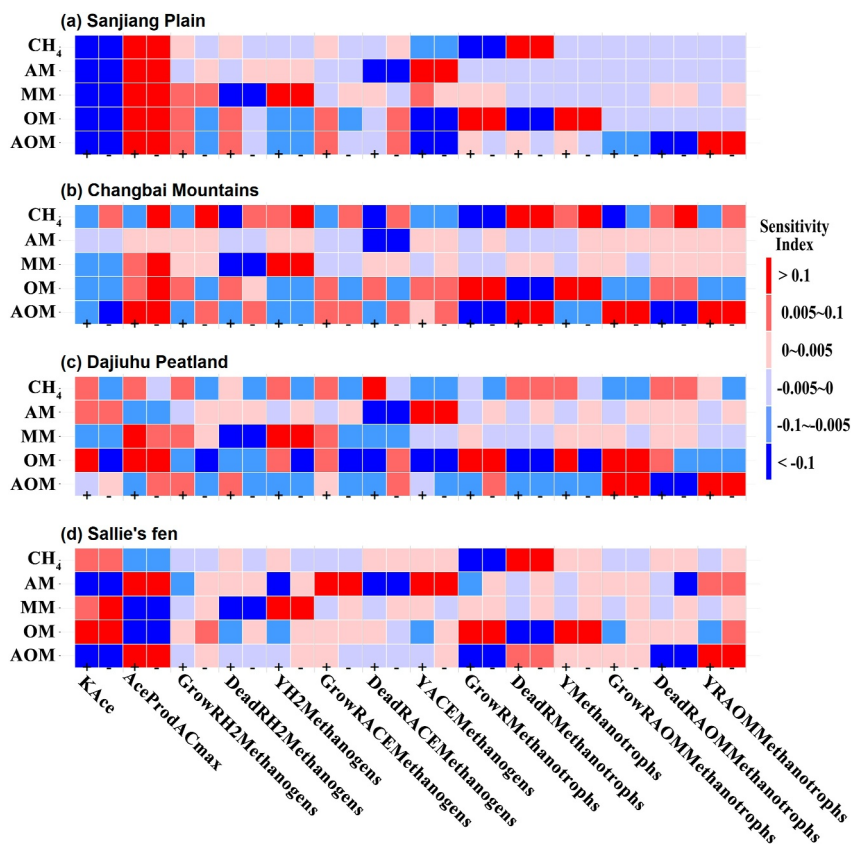


Figure 5. Sensitivity analysis of the CLM-Microbe model in terms of CH_4 flux, AM, MM, OM, and AOM to 14 parameters (Table 2) (K_{Ac} , AceProd , AC_{max} , GrowAce , Methanogens , GrowH2 , Methanogens , DeadH2 , Methanogens , YH2 , Methanogens , DeadR , Methanotrophs , YAc , Methanogens , YH2 , Methanogens , DeadR , Methanotrophs , GrowR , Methanotrophs , DeadRA , OM , Methanotrophs , YRA , OM , Methanotrophs) for (a) Sanjiang Plain, (b) Changbai Mountain, (c) Dajiuju Peatland, and (d) Sallie's fen. The symbols "+" and "-" indicate a 20% increase or 20% decrease of parameter values. Darker red and darker blue indicate a stronger positive or negative model response to a parameter change, respectively. S is negative if the direction of model response opposes the direction of a parameter change, and vice versa.

underscored the substantial influence of acetate on CH_4 flux, which is consistent with our research (James, 1993; Segers, 1998).

The substrates and CH_4 production are crucial factors regulating the temporal patterns of CH_4 (Ricciuto et al., 2021). In this study, not only parameters related to CH_4 substrates but also those controlling CH_4 microbial growth and death rates, as well as growth efficiency, are crucial in affecting CH_4 flux in this study (Figure 5). Previous research has confirmed that microorganism growth and death rates are the primary drivers controlling CH_4 flux (Tiedje et al., 2022). An increase in microbial growth rate typically results in higher CH_4 production rates, while increasing microbial death rate may reduce CH_4 consumption speed (Kroeger et al., 2021). In particular, for the simulation at the Sanjiang Plain, we adjusted parameters related to hydrogenotrophic methanogens to increase methanogen abundance (Figure 5, Table 2), which enhanced CH_4 production rates via the hydrogenotrophic pathway (Figure 1). Therefore, adjusting these parameters can notably impact the seasonal distribution of CH_4 flux. Furthermore, changing the parameters for microbial growth and death rates is vital for simulating CH_4 flux variations under different environmental conditions (Ricciuto et al., 2021; Zuo et al., 2022). Diverse ecosystems or habitats may host distinct microbial communities and environmental conditions; hence, parameter adjustments to accommodate these variations are crucial (Sihl et al., 2021; Song et al., 2020).

4.3. Implications

Integrating gene data with wetland CH_4 models is profoundly meaningful for several reasons. Firstly, integrating genetic data with CH_4 models optimized CH_4 microbial process parameters, improving the seasonal variation

trends of CH_4 production rates and enhancing the accuracy of CH_4 flux simulations (Figure 2). In a few models that include microbial CH_4 production processes, the lack of data for parameterizing these processes hindered model optimization (Ricciuto et al., 2021). For instance, the JULES model introduced CH_4 -producing bacteria growth and dormancy processes, resulting in an approximately 12% increase in CH_4 emissions (Chadburn et al., 2020); the TEM model, by incorporating CH_4 -producing bacteria and CH_4 -oxidizing bacteria into key model processes, found that CH_4 uptake nearly doubled (Oh et al., 2020). Therefore, integrating gene data with CH_4 models is crucial for understanding wetland CH_4 microbial processes and model development.

Second, integrating gene data and modeling methods enables us to gain a mechanistic understanding of microbial CH_4 production and its responses to the environment in wetland ecosystems. In this study, the application of gene data allowed us to optimize the season trends of CH_4 production rates, reveal the vertical trends of methanogens, and explore the relationships between various environmental factors and CH_4 production rates (Figures 1, 3 and 4). Microbes are pivotal players in wetlands, significantly influencing CH_4 flux (Iqbal et al., 2019; Tiwari et al., 2020). Through the lens of gene data, we can decipher how different microbial communities respond to environmental changes (Arnold et al., 2023). This knowledge grants us a more profound understanding of the intricate mechanisms governing CH_4 cycling in these ecosystems. Consequently, it reveals the functions and interactions of microbes within ecosystems, further enriching our ecological insights into wetlands.

Lastly, integrating functional gene data with wetland CH_4 models plays a vital role in bridging knowledge gaps in the field of research. The dynamics of wetland CH_4 cycling represent a complex ecological process, and previous models have often considered only limited factors. Gene data steps in to provide a more comprehensive data source, aiding in the establishment of ecosystem-scale predictability. This predictability is founded on site-specific observation data and micro-scale omics datasets (Xu & Rodrigues, 2023). As a result, this integration enhances model parameterization based on omics data and ecosystem-scale CH_4 flux, and concurrently, it offers pivotal insights into addressing broader climate and environmental issues.

4.4. Limitations

This study demonstrated that genome-enabled model parameterization enhances the performance of the CLM-Microbe model in simulating microbial mechanisms for CH_4 cycling in four natural wetlands. We identified four key limitations that will be addressed in future work. First, the dormancy of methanogens and methanotrophs was not considered; previous research has shown that the dormant methanogen population constitutes a significant portion (Liu et al., 2011; Thauer, 1998), although active biomass generally explains seasonal variations in CH_4 flux (King, 1994). Second, the consistency of functional gene measurement will likely reduce the bias of the present study. The wetland in the Sanjiang Plain used shotgun metagenomic sequencing, while the other three sites relied on 16S rRNA sequencing. Although clustering analysis of 16S rRNA sequences provides information on microbial community composition, it poses limitations in distinguishing strains involved in different CH_4 production pathways, as most CH_4 producers can utilize both acetate and CO_2 (Angle et al., 2017). On the other hand, shotgun metagenomic sequencing directly differentiates functional gene abundances associated with distinct pathways by analyzing comprehensive genomic functional information and comparing it with databases (Wang, Zhu, et al., 2022). Third, while the CLM-Microbe model considers the impact of methanotrophy on CH_4 cycling, this study needed to validate the methanotrophy biomass due to the scarcity of methanotrophy data. Some studies have suggested that explicitly considering methanotrophy biomass can improve the simulation of seasonal CH_4 flux (Murguia-Flores et al., 2018; Xu, Riley, et al., 2016). The lack of functional gene data for methanotrophs prevents a robust parameterization in this study on the CH_4 oxidation, which might manifest as significant biases in the spatiotemporal dynamics of simulated CH_4 flux (Barney et al., 2024). Therefore, we recommend that future research focus on collecting as much measurement data as possible and further exploring the potential of integrating gene data. Despite the explicit representation of methanogens and methanotrophs allowing the CLM-Microbe model to simulate the CH_4 biomass of those microbes, current model parameterization limits relative changes in those functional microbes, resulting in considerable uncertainties when estimating CH_4 fluxes (Figure 3).

5. Conclusions

This study reported a new approach to fusing functional gene data with the CLM-Microbe model to adjust the parameters to reach a better model simulation of CH_4 flux at the site level. Additional constraints of gene data

improved the simulation accuracy of seasonal variations in CH_4 flux and captured relative trends in methanogen microbial biomass. Sensitivity analysis revealed that growth and mortality rates of methanogens are critical parameters controlling CH_4 flux and microbial biomass. Furthermore, genome-driven parameterization further enhanced the CLM-Microbe model in reproducing the seasonal variability of CH_4 production rates through different pathways. Additionally, the integration of gene data with the model has strengthened the relationship between microbial CH_4 production processes, specifically acetoclastic methanogenesis and hydrogenotrophic methanogenesis, and environmental factors such as soil temperature and moisture, thereby enhancing the understanding of microbial mechanisms involved in CH_4 production processes. The genome-enabled parameterization of the microbial-explicit model CLM-Microbe represents a pioneering effort to link gene data with ecosystem function. Explicit representation of CH_4 microbial processes in the CLM-Microbe model will deepen our mechanistic understanding of wetland ecosystem CH_4 cycling and improve predictability of microbial community structures from regional to global scales, thus reducing uncertainties in global carbon projection.

Data Availability Statement

Model forcing, output data, and observational methane flux data are available through the Zenodo data repository: <https://doi.org/10.5281/zenodo.11127249> (Zuo et al., 2024). The CLM-Microbe model code can be found at Github: <https://github.com/email-clm/CLM-Microbe> (Xu et al., 2022).

Acknowledgments

This study was partially supported by the National Natural Science Foundation of China (42330509, 42220104009 and 42293263), the National Key R&D Program of China (2023YFF0807202), the Strategic Priority Research Program of the Chinese Academy of Sciences (XDA28020502), the China Postdoctoral Science Foundation (2024M753211), and the Ecology Innovation Team (2020CXTD02) at Minzu University of China. X.X., L.H., and Y.W. are grateful for the financial and facility support from San Diego State University and the U.S. National Science Foundation (2145130) in improving the CLM-Microbe model. Additionally, the study acknowledges support from The Young Scientists Innovation Funds of State Key Laboratory of Black Soils Conservation and Utilization (2023HTDGZ-QN-03) and the Jilin Provincial Natural Science Foundation to N.C. (YDZJ202201ZYTS477).

References

Angle, J. C., Morin, T. H., Soden, L. M., Narro, A. B., Smith, G. J., Borton, M. A., et al. (2017). Methanogenesis in oxygenated soils is a substantial fraction of wetland methane emissions. *Nature Communications*, 8(1), 1567. <https://doi.org/10.1038/s41467-017-01753-4>

Arnold, W., Taylor, M., Bradford, M., Raymond, P., & Peccia, J. (2023). Microbial activity contributes to spatial heterogeneity of wetland methane fluxes. *Microbiology Spectrum*, 0(0), e02714. <https://doi.org/10.1128/spectrum.02714-23>

Bajic, D., & Sanchez, A. (2020). The ecology and evolution of microbial metabolic strategies. *Current Opinion in Biotechnology*, 62, 123–128. <https://doi.org/10.1016/j.copbio.2019.09.003>

Barney, M., Hopple, A. M., Gregory, L. L., Keller, J. K., & Bridgman, S. D. (2024). Anaerobic oxidation of methane mitigates net methane production and responds to long-term experimental warming in a northern bog. *Soil, Biology and Biochemistry*, 190, 109316. <https://doi.org/10.1016/j.soilbio.2024.109316>

Blanco, J. A., Seely, B., Welham, C., Kimmens, J. P., & Seebacher, T. M. (2007). Testing the performance of a forest ecosystem model (FORECAST) against 29 years of field data in a *Pseudotsuga menziesii* plantation. *Canadian Journal of Forest Research*, 37(10), 1808–1820. <https://doi.org/10.1139/x07-041>

Cao, N. (2015). *Study on the carbon dioxide flux in Peatland of volcanic cluster in the longgang region at changbai mountain—Take the Jinchuan peatland as an example*. Northeast Normal University.

Chadburn, S. E., Aalto, T., Aurela, M., Baldocchi, D., Biasi, C., Boike, J., et al. (2020). Modeled microbial dynamics explain the apparent temperature sensitivity of wetland methane emissions. *Global Biogeochemical Cycles*, 34(11), e2020GB006678. <https://doi.org/10.1029/2020gb006678>

Chen, H., Zhu, T., Li, B., Fang, C., & Nie, M. (2020). The thermal response of soil microbial methanogenesis decreases in magnitude with changing temperature. *Nature Communications*, 11(1), 5733. <https://doi.org/10.1038/s41467-020-19549-4>

Church, D. L., Cerutti, L., Gürler, A., Griener, T., Zelazny, A., & Emmer, S. (2020). Performance and application of 16S rRNA gene cycle sequencing for routine identification of bacteria in the clinical microbiology laboratory. *Clinical Microbiology Reviews*, 33(4). <https://doi.org/10.1128/cmr.00053-19>

Dellageneze, B. M., Bovio-Winkler, P., Lavergne, C., Menoni, D. A., Mosquillo, F., Cabrol, L., et al. (2023). Acetoclastic archaea adaptation under increasing temperature in lake sediments and wetland soils from Alaska. *Polar Biology*, 46(4), 259–275. <https://doi.org/10.1007/s00300-023-03120-0>

Fazli, P., Man, H. C., Shah, U. K. M., & Idris, A. (2013). Characteristics of methanogens and methanotrophs in rice fields: A review. *Asia-Pacific Journal of Molecular Biology and Biotechnology*, 21(1), 3–17.

Forster, P. (2007). Changes in atmospheric constituents and in radiative forcing. In *Climate change 2007: The Physical Science Basis. Contribution of working Group I to the Fourth Assessment Report of the Intergovernmental Panel on climate change*, 2007.

He, L., Lai, C. T., Mayes, M. A., Murayama, S., & Xu, X. (2021). Microbial seasonality promotes soil respiratory carbon emission in natural ecosystems: A modeling study. *Global Change Biology*, 27(13), 3035–3051. <https://doi.org/10.1111/gcb.15627>

He, L., Lipson, D. L., Rodrigues, J. L., Mayes, M. A., Bjork, R. G., Glaser, B., et al. (2021). Dynamics of fungal and bacterial biomass carbon in natural ecosystems: Site-level applications of the CLM-microbe model. *Journal of Advances in Modeling Earth Systems*, 13, e2020MS002283. <https://doi.org/10.1029/2020MS002283>

Hines, M. E., Duddleston, K. N., Rooney-Varga, J. N., Fields, D., & Chanton, J. P. (2008). Uncoupling of acetate degradation from methane formation in Alaskan wetlands: Connections to vegetation distribution. *Global Biogeochemical Cycles*, 22(2). <https://doi.org/10.1029/2006gb002903>

IPCC. (2021). *Climate change 2021: The Physical Science Basis. Contribution of working group I to the Sixth Assessment Report of the Intergovernmental Panel on climate change*. Cambridge University Press.

Iqbal, A., Shang, Z., Rehman, M. L. U., Ju, M., Rehman, M. M. U., Rafiq, M. K., et al. (2019). Pattern of microbial community composition and functional gene repertoire associated with methane emission from Zoige wetlands, China—A review. *Science of the Total Environment*, 694, 133675. <https://doi.org/10.1016/j.scitotenv.2019.133675>

James, R. T. (1993). Sensitivity analysis of a simulation model of methane flux from the Florida Everglades. *Ecological Modelling*, 68(3), 119–146. [https://doi.org/10.1016/0304-3800\(93\)90013-i](https://doi.org/10.1016/0304-3800(93)90013-i)

Kalyuzhnaya, M. G., Gomez, O. A., & Murrell, J. C. (2019). The methane-oxidizing bacteria (methanotrophs). *Taxonomy, genomics and ecophysiology of hydrocarbon-degrading microbes*, 245–278. https://doi.org/10.1007/978-3-030-14796-9_10

Kharitonov, S., Semenov, M., Sabrekov, A., Kotsyurbenko, O., Zhelezova, A., & Schegolkova, N. (2021). Microbial communities in methane cycle: Modern molecular methods gain insights into their global ecology. *Microbial Communities in Methane Cycle: Modern Molecular Methods Gain Insights into Their Global Ecology*. *Environments*, 8(2), 16. <https://doi.org/10.3390/environments8020016>

King, G. M. (1994). Associations of methanotrophs with the roots and rhizomes of aquatic vegetation. *Applied and Environmental Microbiology*, 60(9), 3220–3227. <https://doi.org/10.1128/aem.60.9.3220-3227.1994>

Kirschke, S., Bousquet, P., Ciais, P., Saunois, M., Canadell, J. G., Dlugokencky, E. J., et al. (2013). Three decades of global methane sources and sinks. *Nature Geoscience*, 6(10), 813–823. <https://doi.org/10.1038/geo1955>

Koven, C. D., Riley, W. J., Subin, Z. M., Tang, J. Y., Torn, M. S., Collins, W. D., et al. (2013). The effect of vertically resolved soil biogeochemistry and alternate soil C and N models on C dynamics of CLM4. *Biogeosciences*, 10(11), 7109–7131. <https://doi.org/10.5194/bg-10-7109-2013>

Kroeger, M. E., Meredith, L. K., Meyer, K. M., Webster, K. D., De Camargo, P. B., De Souza, L. F., et al. (2021). Rainforest-to-pasture conversion stimulates soil methanogenesis across the Brazilian Amazon. *The ISME Journal*, 15(3), 658–672. <https://doi.org/10.1038/s41396-020-00804-x>

Liu, D. Y., Ding, W. X., Jia, Z. J., & Cai, Z. C. (2011). Relation between methanogenic archaea and methane production potential in selected natural wetland ecosystems across China. *Biogeosciences*, 8(2), 329–338. <https://doi.org/10.5194/bg-8-329-2011>

Liu, Y., Ge, J., Sinan, Y., Jiang, H., Yuan, H., Feng, L., et al. (2021). Variation characteristics of methane flux and its relationship with the composition of methanogens in the subalpine peat wetland of Dajihu, Shennongjia. *Resources and Environment in the Yangtze Basin*, 30(06), 1418–1427.

Melton, J. R., Wania, R., Hodson, E. L., Poulter, B., Ringeval, B., Spahni, R., et al. (2013). Present state of global wetland extent and wetland methane modelling: Conclusions from a model inter-comparison project (WETCHIMP). *Biogeosciences*, 10(2), 753–788. <https://doi.org/10.5194/bg-10-753-2013>

Murguia-Flores, F., Arndt, S., Ganesan, A. L., Murray-Tortarolo, G., & Hornibrook, E. R. (2018). Soil methanotrophy model (MeMo v1.0): A process-based model to quantify global uptake of atmospheric methane by soil. *Geoscientific Model Development*, 11(6), 2009–2032. <https://doi.org/10.5194/gmd-11-2009-2018>

Nazaries, L., Murrell, J. C., Millard, P., Baggs, L., & Singh, B. K. (2013). Methane, microbes and models: Fundamental understanding of the soil methane cycle for future predictions. *Environmental Microbiology*, 15(9), 2395–2417. <https://doi.org/10.1111/1462-2920.12149>

Noyce, G. L., Varner, R. K., Bubier, J. L., & Frolking, S. (2014). Effect of Carex rostrata on seasonal and interannual variability in peatland methane emissions. *Journal of Geophysical Research: Biogeosciences*, 119(1), 24–34. <https://doi.org/10.1002/2013jg002474>

Oh, Y., Zhuang, Q., Liu, L., Welp, L. R., Lau, M. C., Onstott, T. C., et al. (2020). Reduced net methane emissions due to microbial methane oxidation in a warmer Arctic. *Nature Climate Change*, 10(4), 317–321. <https://doi.org/10.1038/s41558-020-0734-z>

Perryman, C. R., McCalley, C. K., Ernakovich, J. G., Lamit, L. J., Shorter, J. H., Lilleskov, E., & Varner, R. K. (2022). Microtopography matters: Belowground CH₄ cycling regulated by differing microbial processes in peatland hummocks and lawns. *Journal of Geophysical Research: Biogeosciences*, 127(8), e2022JG006948. <https://doi.org/10.1029/2022JG006948>

Reid, A. (2011). *Incorporating microbial processes into climate models: Report on an American Academy of Microbiology Colloquium held on Feb. 21–23, 2011*. American Society for Microbiology.

Ricciuto, D. M., Xu, X., Shi, X., Wang, Y., Song, X., Schadt, C. W., et al. (2021). An integrative model for soil biogeochemistry and methane processes: I. Model structure and sensitivity analysis. *Journal of Geophysical Research: Biogeosciences*, 126(8), e2019JG005468. <https://doi.org/10.1029/2019JG005468>

Segers, R. (1998). Methane production and methane consumption: A review of processes underlying wetland methane fluxes. *Biogeochemistry*, 41(1), 23–51. <https://doi.org/10.1023/a:1005929032764>

Sharp, S. J., Maietta, C. E., Stewart, G. A., Taylor, A. K., Williams, M. R., & Palmer, M. A. (2024). Net methane production predicted by patch characteristics in a freshwater wetland. *Journal of Geophysical Research: Biogeosciences*, 129(1), e2023JG007814. <https://doi.org/10.1029/2023JG007814>

Shi, Y. (2019). *Effects of nitrogen input on carbon and nitrogen transformations in peatlands*. Doctor Thesis. Northeast Normal University.

Sihi, D., Xu, X., Salazar Ortiz, M., O'Connell, C. S., Silver, W. L., López-Lloreda, C., et al. (2021). Representing methane emissions from wet tropical forest soils using microbial functional groups constrained by soil diffusivity. *Biogeosciences*, 18(5), 1769–1786. <https://doi.org/10.5194/bg-18-1769-2021>

Song, C., Luan, J., Xu, X., Ma, M., Aurela, M., Lohila, A., et al. (2020). A microbial functional group-based CH₄ model integrated into a terrestrial ecosystem model: Model structure, site-level evaluation, and sensitivity analysis. *Journal of Advances in Modeling Earth Systems*, 12(4), e2019MS001867. <https://doi.org/10.1029/2019ms001867>

Sulman, B. N., Moore, J. A., Abramoff, R., Averill, C., Kivlin, S., Georgiou, K., et al. (2018). Multiple models and experiments underscore large uncertainty in soil carbon dynamics. *Biogeochemistry*, 141(2), 109–123. <https://doi.org/10.1007/s10533-018-0509-z>

Sulman, B. N., Phillips, R. P., Oishi, A. C., Sheviakova, E., & Pacala, S. W. (2014). Microbe-driven turnover offsets mineral-mediated storage of soil carbon under elevated CO₂. *Nature Climate Change*, 4(12), 1099–1102. <https://doi.org/10.1038/nclimate2436>

Thauer, R. K. (1998). Biochemistry of methanogenesis: A tribute to Marjory Stephenson: 1998 Marjory Stephenson prize lecture. *Microbiology*, 144(9), 2377–2406. <https://doi.org/10.1099/00221287-144-9-2377>

Theil, H. (1966). *Applied economic forecasting*. North-Holland.

Thornton, P. E., & Rosenbloom, N. A. (2005). Ecosystem model spin-up: Estimating steady state conditions in a coupled terrestrial carbon and nitrogen cycle model. *Ecological Modelling*, 189(1–2), 25–48. <https://doi.org/10.1016/j.ecolmodel.2005.04.008>

Tiedje, J. M., Bruns, M. A., Casadevall, A., Criddle, C. S., Elsie-Fadrosh, E., Karl, D. M., et al. (2022). Microbes and climate change: A research Prospectus for the future. *Mbio. mBio*, 13(3), e00800–e00822. <https://doi.org/10.1128/mbio.00800-22>

Tiwari, S., Singh, C., & Singh, J. S. (2020). Wetlands: A major natural source responsible for methane emission. *Restoration of Wetland Ecosystem: A Trajectory Towards a Sustainable Environment*, 59–74. https://doi.org/10.1007/978-981-13-7665-8_5

Tootchi, A., Jost, A., & Ducharme, A. (2019). Multi-source global wetland maps combining surface water imagery and groundwater constraints. *Earth System Science Data*, 11(1), 189–220. <https://doi.org/10.5194/essd-11-189-2019>

Ueyama, M., Knox, S. H., Delwiche, K. B., Bansal, S., Riley, W. J., Baldocchi, D., et al. (2023). Modeled production, oxidation, and transport processes of wetland methane emissions in temperate, boreal, and Arctic regions. *Global Change Biology*, 29(8), 2313–2334. <https://doi.org/10.1111/geb.16594>

Ueyama, M., Yazaki, T., Hirano, T., & Ryosuke, E. (2022). Partitioning methane flux by the eddy covariance method in a cool temperate bog based on a Bayesian framework. *Agricultural and Forest Meteorology*, 316, 108852. <https://doi.org/10.1016/j.agrformet.2022.108852>

Walker, T. W., Kaiser, C., Strasser, F., Herbold, C. W., Leblans, N. I. W., Woebken, D., et al. (2018). Microbial temperature sensitivity and biomass change explain soil carbon loss with warming. *Nature Climate Change*, 8(10), 885–889. <https://doi.org/10.1038/s41558-018-0259-x>

Wang, N., Zhu, X., Zuo, Y., Liu, J., Yuan, F., Guo, Z., et al. (2022). Metagenomic evidence of suppressed methanogenic pathways along soil profile after wetland conversion to cropland. *Frontiers in Microbiology*, 13, 930694. <https://doi.org/10.3389/fmicb.2022.930694>

Wang, Y., Yuan, F., Arndt, K. A., Liu, J., He, L., Zuo, Y., et al. (2022). Upscaling methane flux from Plot level to eddy covariance tower domains in five Alaskan Tundra ecosystems. *Frontiers in Environmental Science*, 10, 939238. <https://doi.org/10.3389/fenvs.2022.939238>

Wang, Y., Yuan, F., Yuan, F., Gu, B., Hahn, M. S., Torn, M. S., et al. (2019). Mechanistic modeling of microtopographic impacts on CO₂ and CH₄ fluxes in an Alaskan Tundra ecosystem using the CLM-Microbe model. *Journal of Advances in Modeling Earth Systems*, 11(12), 4288–4304. <https://doi.org/10.1029/2019ms001771>

Xu, X., Elias, D. A., Graham, D. E., Phelps, T. J., Carroll, S. L., Wullschleger, S. D., & Thornton, P. E. (2015). A microbial functional group-based module for simulating methane production and consumption: Application to an incubated permafrost soil. *Journal of Geophysical Research: Biogeosciences*, 120(7), 1315–1333. <https://doi.org/10.1002/2015jg002935>

Xu, X., He, L., & Wang, Y. (2022). CLM-Microbe v1.0. *Zenodo*. <https://doi.org/10.5281/zenodo.7439312>

Xu, X., Riley, W. J., Koven, C. D., Billesbach, D. P., Chang, R. Y. W., Commane, R., et al. (2016). A multi-scale comparison of modeled and observed seasonal methane emissions in northern wetlands. *Biogeosciences*, 13(17), 5043–5056. <https://doi.org/10.5194/bg-13-5043-2016>

Xu, X., & Rodrigues, J. (2023). Scaling genes to global methane modeling through artificial intelligence.

Xu, X., Schimel, J. P., Thornton, P. E., Song, X., Yuan, F., & Goswami, S. (2014). Substrate and environmental controls on microbial assimilation of soil organic carbon: A framework for Earth system models. *Ecology Letters*, 17(5), 547–555. <https://doi.org/10.1111/ele.12254>

Xu, X., Yuan, F., Hanson, P. J., Wullschleger, S. D., Thornton, P. E., Riley, W. J., et al. (2016). Reviews and syntheses: Four decades of modeling methane cycling in terrestrial ecosystems. *Biogeosciences Discussions*, 13(12), 3735–3755. <https://doi.org/10.5194/bg-13-3735-2016>

Yuan, F., Wang, Y., Ricciuto, D. M., Shi, X., Yuan, F., Hanson, P. J., et al. (2021). An integrative model for soil biogeochemistry and methane processes: II. Warming and elevated CO₂ effects on peatland CH₄ emissions. *Journal of Geophysical Research: Biogeosciences*, 126(8). <https://doi.org/10.1029/2020jg005963>

Yuan, F., Wang, Y., Ricciuto, D. M., Shi, X., Yuan, F., Brehme, T., et al. (2021). Hydrological Feedbacks on peatland CH₄ emission under warming and elevated CO₂: A modeling study. *Journal of Hydrology*, 603, 127137. <https://doi.org/10.1016/j.jhydrol.2021.127137>

Zuo, Y., He, L., Wang, Y., Liu, J., Wang, N., Li, K., et al. (2024). Genome-enabled parameterization enhances model simulation of CH₄ cycling in four natural wetlands (CLM-Microbe) [Dataset]. *Zenodo*. <https://doi.org/10.5281/zenodo.11127249>

Zuo, Y., Wang, Y., He, L., Wang, N., Liu, J., Yuan, F., et al. (2022). Modeling methane dynamics in three wetlands in Northeastern China by using the CLM-Microbe model. *Ecosystem Health and Sustainability*, 8(1), 2074895. <https://doi.org/10.1080/20964129.2022.2074895>

References From the Supporting Information

He, L., Viovy, N., & Xu, X. (2023). Macroecology differentiation between bacteria and fungi in topsoil across the United States. *Global Biogeochemical Cycles*, 37(11), e2023GB007706. <https://doi.org/10.1029/2023GB007706>

Vanclay, J. K., & Skovsgaard, J. P. (1997). Evaluating forest growth models. *Ecological Modelling*, 98(1), 1–12. [https://doi.org/10.1016/S0304-3800\(96\)01932-1](https://doi.org/10.1016/S0304-3800(96)01932-1)